

# Connexin43 ablation in foetal atrial myocytes decreases electrical coupling, partner connexins, and sodium current

Thomas Desplantez<sup>1</sup>, Megan L. McCain<sup>2</sup>, Philippe Beauchamp<sup>1</sup>, Ghislaine Rigoli<sup>1</sup>, Barbara Rothen-Rutishauser<sup>3</sup>, Kevin Kit Parker<sup>2</sup>, and Andre G. Kleber<sup>1\*</sup>

<sup>1</sup>Department of Physiology, University of Bern, Bern, Switzerland; <sup>2</sup>Disease Biophysics Group, School of Engineering and Applied Sciences, Harvard University, Cambridge, MA, USA; and <sup>3</sup>Department of Anatomy, University of Bern, Bern, Switzerland

Received 20 December 2010; revised 10 January 2012; accepted 23 January 2012; online publish-ahead-of-print 27 January 2012

Time for primary review: 22 days

**Aims** Remodelling and regional gradients in expression of connexins (Cx) are thought to contribute to atrial electrical dysfunction and atrial fibrillation. We assessed the effect of interaction between Cx43, Cx40, and Cx45 on atrial cell-to-cell coupling and inward Na current ( $I_{Na}$ ) in engineered pairs of atrial myocytes derived from wild-type mice (Cx43<sup>+/+</sup>) and mice with genetic ablation of Cx43 (Cx43<sup>-/-</sup>).

**Methods and results** Cell pairs were engineered by microcontact printing from atrial Cx43<sup>+/+</sup> and Cx43<sup>-/-</sup> murine myocytes (1 day before birth, 3–5 days in culture). Dual and single voltage clamp were used to measure intercellular electrical conductance,  $g_j$ , and its dependence on transjunctional voltage,  $V_j$ , single gap junction channel conductances, and  $I_{Na}$ . 3D reconstructions of Cx43, Cx40, and Cx45 immunosignals in gap junctions were made from confocal slices.

Full genetic Cx43 ablation produced a decrease in immunosignals of Cx40 to  $62 \pm 10\%$  (mean  $\pm$  SE;  $n = 17$ ) and Cx45 to  $66 \pm 8\%$  ( $n = 16$ ).  $G_j$  decreased from  $80 \pm 9$  nS (Cx43<sup>+/+</sup>,  $n = 17$ ) to  $24 \pm 2$  nS (Cx43<sup>-/-</sup>,  $n = 35$ ). Single channel analysis showed a shift in the main peak of the channel histogram from  $49 \pm 1.7$  nS (Cx43<sup>+/+</sup>) to  $67 \pm 1.8$  nS (Cx43<sup>-/-</sup>) with a second minor peak appearing at  $27 \pm 1.5$  pS. The dependence of  $g_j$  on  $V_j$  decreased with Cx43 ablation. Importantly, peak  $I_{Na}$  decreased from  $-350 \pm 44$  pA/pF (Cx43<sup>+/+</sup>) to  $-154 \pm 28$  pA/pF (Cx43<sup>-/-</sup>).

**Conclusions** The dependence of Cx40, Cx45, and  $I_{Na}$  on Cx43 expression indicates a complex interaction between connexins and  $I_{Na}$  in the atrial intercalated discs that is likely to be of relevance for arrhythmogenesis.

**Keywords** Connexin • Atrial cell-to-cell coupling • Cx43 ablation • Sodium current

## 1. Introduction

Normal cardiac function requires coordinated and rapid electrical excitation and contraction. It involves a complex interface machinery between myocytes consisting of fascia adherens junctions and desmosomes linking the micro- and intermediate filaments between cells, and the gap junctions that provide low-resistance pathways for electrical current and pores for molecular cross-talk. Na<sup>+</sup> channels contributing to electrical excitation are clustered, at least in part, in the cellular interface and are affected by desmosomal mutations.<sup>1–4</sup>

Connexins that form the protein subunits of gap junction channels are known to be specifically distributed in cardiac regions.<sup>5</sup> In atrial myocardium, connexin43 (Cx43) and Cx40 are the prominent connexins. Moreover, Cx45 has been described in small amounts in atria of mice, rats, and humans.<sup>6–9</sup> The distribution of these connexins seems to be non-uniform in atrial tissue, with a more prominent presence of Cx40 in the right than in the left atrium. In pathological settings, remodelling of atrial connexins has been described that varies according to the experimental model and species used. Moreover, inhomogeneity of connexin expression with local gradients in Cx43

\* Corresponding author. Department of Pathology, Beth Israel Deaconess Medical Center, Harvard Medical School, Boston, 02215 MA, USA. Tel: +1 617 599 8222; fax: +1 617 677 2943, Email: akleber@bidmc.harvard.edu

and Cx40 distribution has been implicated in arrhythmogenesis.<sup>5,10,11</sup> The importance of Cx43 as an atrial connexin has recently been underlined by the description of lone atrial fibrillation associated with a somatic Cx43 mutation.<sup>12</sup>

In previous work, using engineered strands of atrial myocytes in culture, we have shown that genetic Cx43 ablation decreases and Cx40 ablation increases atrial propagation velocity. These electrical changes were not only attributed to the genetic deletion of a given atrial connexin *per se*, but also to the observation that the expression of Cx40 in atrial gap junctions was decreased with Cx43 ablation, and inversely, Cx43 expression in atrial gap junctions was increased with Cx40 ablation.<sup>13</sup> These findings suggested a complex mechanism of atrial remodelling with genetic deletion of Cx43 or Cx40, involving mutual feedback interactions between gap junctional Cx40 and Cx43 expression on the one hand, and a potential role of a change in the Cx mixture and electrical conductances of gap junction channels on the other. Characterization of heterotypic and heteromeric gap junction channels composed of Cx43, Cx40, and Cx45 thus far has been investigated in heterologous expression systems (see<sup>14–16</sup> for review). In general, it is known that Cx45 can form heteromeric connexons and heterotypic gap junction channels with Cx43 or Cx40. The formation of heteromeric Cx43/Cx40 connexons may occur, but the resulting gap junction channels are of low electrical conductance and density.<sup>17,18</sup>

In this work, our goal was to define the change in the electrical properties of atrial cell junctions with genetic Cx43 ablation and analyse the changes of the partner connexins, Cx40 and Cx45. To enable stable dual voltage clamp recordings of the gating behaviour of gap junctions and single channel openings, we used engineered pairs of atrial cells. Engineering also produced accurately defined cell junctions that enabled high-resolution imaging and quantification of Cx immunosignals in gap junctions.

## 2. Methods

### 2.1. Culture and engineering of atrial cell pairs

Before removal of the hearts at 1 day before birth (D-1), animals were deeply anaesthetized with CO<sub>2</sub> and rapidly decapitated. All animal experiments and procedures were approved by the Swiss Federal and Bernese Veterinary Offices and conform to the *Guide for the Care and Use of Laboratory Animals* published by the US national institute of Health (NIH Publication No. 85–23, revised 1996). The excision of atrial tissue was strictly limited to the right and left auricles. This excludes contamination by tissue from the sino-atrial or atrio-ventricular nodes. The procedure to harvest murine atrial myocytes and the preplating procedure has been described in detail.<sup>13</sup> Also, we have previously shown that there is no difference in electrical phenotype between Cx43<sup>+/+</sup> murine myocytes harvested at D-1 or D1 after 3–4 days in culture.<sup>13</sup> Coverslips were covered with a fibronectin pattern of predefined geometry using soft-microlithography.<sup>19</sup> In brief, PDMS (polydimethylsiloxane) stamps were prepared in such a way that the profile on the stamps formed rectangular islands. PDMS stamps were coated with 25 µg/mL fibronectin, and the fibronectin was transferred from the fibronectin-coated stamps to the PDMS-coated coverslips. After cell seeding, cell-to-cell contacts established gap junctions within 24 h, as verified by dual voltage clamp. As illustrated in *Figure 1*, the atrial pairs showed a longitudinal shape and a well-defined cell-to-cell interface located at the fibronectin-free gap (width 2 µm) between two fibronectin rectangles. The height of the atrial cell pairs varied from 5 to 7 µm (see Supplementary material online).

### 2.2. Immunohistochemistry and confocal laser scanning microscopy

Immunofluorescence staining was performed for Cx43, Cx40, and Cx45. In a small number of experiments, immunofluorescence signals for N-cadherin (a protein of the fascia adherens junctions) were obtained.

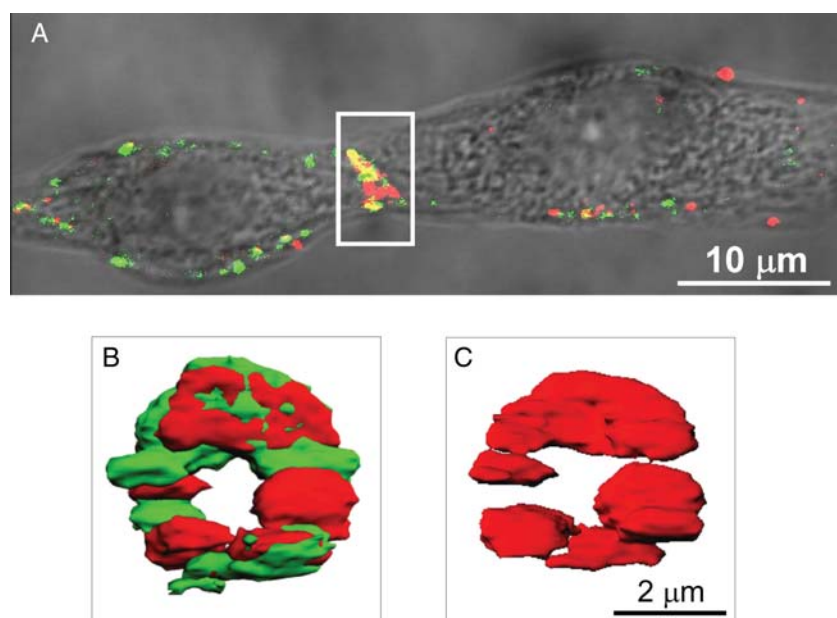


**Figure 1** Engineered atrial cell pair. (A) Wide Field image of engineered murine atrial cell Cx43<sup>+/+</sup> pair overlaid with the immunofluorescence of N-Cadherin (green) and Cx40 (red). Note the sharply defined interface between the two myocytes (*x/z* plane). (B) 3D surface rendering of N-Cadherin (green) and Cx40 (red) immunofluorescence signals shown in the *y/z* plane. (C) 3D surface rendering of Cx40 immunofluorescence signal alone showing plaque-like arrangement of Cx40. Image deconvolution was applied to confocal signals before reconstruction.

Immunostained cells were imaged with a Zeiss LSM 510 META confocal laser scanning microscope at  $\times 100$  magnification. Individual confocal slices were deconvolved using Huygens Essential (Scientific Volume Imaging). Images were analysed using Imaris (Bitplane, Inc., Switzerland). Junctional Cx43, Cx40, and Cx45 were determined from 3D reconstructions of the immunosignals (Figure 1). As shown in Figure 1, the cell junctions formed clearly circumscribed interfaces between the rectangular cells, where connexins were closely associated with N-cadherin (see Supplementary material online for details).

### 2.3. Whole-cell dual and single voltage

Cells were superfused at room temperature (23°C) in modified Krebs–Ringer solution containing (in mmol/L): 140 NaCl, 4 KCl, 2 CaCl<sub>2</sub>, 1 MgCl<sub>2</sub>, 5 HEPES (pH 7.4) 5 glucose, 2 Na-pyruvate. Patch pipettes were filled with internal solution containing (in mmol/L): 130 K-aspartate, 10 NaCl, 1 CaCl<sub>2</sub>, 10 EGTA (pCa 8.1), 3 MgATP, 5 HEPES (pH 7.2).<sup>20</sup> For whole-cell recordings, pipettes were mounted on a micromanipulator (MP-258, Sutter Instruments, USA) and connected to an amplifier (EPC-10, HEKA Elektronik, Germany). ‘Pulse’ and ‘PulseFit’ software (HEKA Elektronik) were used for data acquisition and analysis; SigmaPlot and SigmaStat (Jandel Scientific, Germany) were used for curve fitting and statistics.

Na current,  $I_{Na}$ , was recorded from single isolated atrial myocytes in the whole-cell configuration (depolarizing pulses of 100 ms duration, holding potential  $-90$ , 10 mV increments), and normalized to cell membrane capacitance,  $C_m$ .

Dual whole-cell voltage clamp was applied to patterned cell pairs as previously described.<sup>20,21</sup> Gap junctional conductance was determined by application of small junctional pulses ( $V_j = 10$  mV) and corrected for access resistance.<sup>22</sup> To determine the dependence of  $g_j$  on  $V_j$ , gap junction current,  $I_j$ , was determined at the beginning ( $I_{j,inst}$ ) and end ( $I_{j,ss}$ ) of conjunctive pulses of increasing amplitude, and the conductances  $g_{j,ss}/g_{j,inst}$  were plotted as  $g_{j,ss}/g_{j,inst} = f(V_j)$ . Curve fitting was done with a modified Boltzmann equation applied separately to the data recorded at negative and positive  $V_j$ .<sup>20,23</sup> From this fit  $V_{j,0}$  ( $V_j$  at which  $g_{j,ss}/g_{j,inst}$  is half-maximally inactivated),  $g_{j,max}$  (maximal normalized conductance) and  $g_{j,min}$  (normalized conductance at large  $V_j$ ) were calculated. To study single channel currents elicited at different  $V_j$  gradients of either polarity, a very low degree of cell-to-cell coupling was produced during washout of heptanol (2.5 mmol/L). Unitary conductance of single gap junction channels,  $\gamma_j = i_j/V_j$ , was calculated from  $V_j$  and the discrete current levels,  $i_j$ , (see Supplementary material online).

### 2.4. Statistics

For comparison of data sets, ANOVA or the non-paired Student’s test were used where appropriate. All data are given in means  $\pm$  SEM.

## 3. Results

### 3.1. Effects of atrial germline Cx43 ablation on intercellular conductance and biophysical properties of atrial gap junctions

Atrial cell pairs seeded on micro-patterned coverslips were used for determination of the effect of genetic Cx43 ablation on macroscopic junctional conductance,  $g_j$ , the overall voltage dependence of the gap junction channels, and the spectrum of unitary conductances of gap junction channels. As illustrated in Figure 2A,  $g_j$  decreased from  $80 \pm 9$  nS ( $n = 17$ ) in Cx43<sup>+/+</sup> atrial cell pairs to  $53 \pm 7$  nS ( $n = 32$ ) in Cx43<sup>+/-</sup> pairs and  $23 \pm 2$  nS ( $n = 35$ ) in Cx43<sup>-/-</sup> pairs

(Cx43<sup>+/+</sup> vs. Cx43<sup>+/-</sup>, Cx43<sup>+/+</sup> vs. Cx43<sup>-/-</sup>, and Cx43<sup>+/-</sup> vs. Cx43<sup>-/-</sup>;  $P < 0.05$ ).

The dependence of  $g_{j,ss}$  on  $V_j$  varied considerably among the different cell pairs and genotypes. The average dependence of  $g_j$  on  $V_j$  is depicted on Figure 2B–D. The parameters obtained from the fit to the modified Boltzmann equation<sup>23</sup> are given in Table 1. They indicate that  $g_j$  became less rectifying with Cx43 ablation. Thus,  $V_{j,0}$  amounted to  $-36.6/65.4$  mV (Cx43<sup>+/+</sup>,  $n = 13$ ), to  $-68.6/83.1$  mV (Cx43<sup>+/-</sup>,  $n = 13$ ), and to  $-61.5/72.3$  mV (Cx43<sup>-/-</sup>,  $n = 14$ ).

The frequency distribution of single channel conductances is illustrated in Figure 3A, C and E. In general, ablation of Cx43 produced a shift of the peak unitary conductance from  $49 \pm 1.7$  pS (Cx43<sup>+/+</sup>,  $n = 649$ ) to  $53 \pm 1.4$  pS (Cx43<sup>+/-</sup>,  $n = 335$ ), and  $67 \pm 1.8$  pS (Cx43<sup>-/-</sup>,  $n = 481$ ) with a second minor peak appearing at  $27.1 \pm 1.5$  nS with full Cx43 ablation. This latter smaller peak is very close to the conductance of homomeric/homotypic Cx45 channels measured in heterologous expression systems.<sup>24</sup> Studies in heterogeneous expression system characterizing the biophysical properties of cardiac connexins indicate that this shift is probably explained by the increasing dominance of Cx40 with Cx43 ablation.<sup>24</sup> To detect the likely presence of homomeric/homotypic gap junction channels, we analysed sweeps in which only one open channel could be detected, as illustrated in Figure 3A–E (see Supplementary material online for methodological details). The presence of homomeric/homotypic channels is usually indicated by an absence of a change in  $\gamma_j$  upon a change in polarity in  $V_j$ , and by the value for  $\gamma_j$  considered typical for a given connexin. This is illustrated on the lower trace of Figure 3D, which depicts a channel with a  $\gamma_j$  of 29–31 pS, typical for Cx45. This analysis suggested that channel openings characteristic for homomeric/homotypic Cx43 channels were observed in 13.5% (Cx43<sup>+/+</sup>) and 7.3% (Cx43<sup>+/-</sup>), for homomeric/homotypic Cx40 channels in 4.9% (Cx43<sup>+/+</sup>), 4.5% (Cx43<sup>+/-</sup>), and 14.9% (Cx43<sup>-/-</sup>), and for homomeric/homotypic Cx45 in 8.7% (Cx43<sup>+/+</sup>), 10.1 (Cx43<sup>+/-</sup>), and 8.6% (Cx43<sup>-/-</sup>), the majority of the channels being of mixed composition. Whereas mixed channels in Cx43<sup>+/+</sup> and Cx43<sup>+/-</sup> genotypes might theoretically be composed of all three connexins, the results indicate the domination of mixed Cx40/Cx45 channels in the Cx43<sup>-/-</sup> pairs.

### 3.2. Total atrial germline Cx43 ablation decreases Na<sup>+</sup> inward current

In ventricular myocardium, it has been shown that a significant fraction of Na<sup>+</sup> channels is expressed in intercalated discs.<sup>1–4</sup> Very recently, it has been shown that conditional ablation of Cx43 in ventricular tissue is associated with a decrease in  $I_{Na}$ .<sup>25</sup> In the present experiments, we tested the hypothesis that genetic ablation of Cx43 in atrial tissue could be associated with a change in inward Na<sup>+</sup> current. Therefore, we performed whole-cell single voltage clamp on cells growing on the fibronectin patches as single cell neighbours of the cell pairs. Cell capacitance, which is usually taken as a measure of cell size, was not different between the groups (Cx43<sup>+/+</sup>,  $12.2 \pm 2.5$  pF;  $n = 12$ ; Cx43<sup>-/-</sup>,  $12.9 \pm 3.1$  pF;  $n = 12$ ) and indicated that cell size was small,  $\sim 25\%$  of adult rat ventricular cardiomyocytes.<sup>4</sup>

The comparison of  $I_{Na}$  between a Cx43<sup>+/+</sup> cell, a Cx43<sup>+/-</sup> cell, and a Cx43<sup>-/-</sup> cell is shown in Figure 4A; the collected data are summarized in Figure 4B. Peak  $I_{Na}$  decreased from  $-324, 7 \pm 47.4$  pA/pF (Cx43<sup>+/+</sup>,  $n = 17$ ) to  $-239.6 \pm 51.6$  pA/pF (Cx43<sup>+/-</sup>;  $n = 10$ ), and  $-146.5 \pm 26.4$  pA/pF (Cx43<sup>-/-</sup>,  $n = 11$ ). The decrease of  $I_{Na}$  with

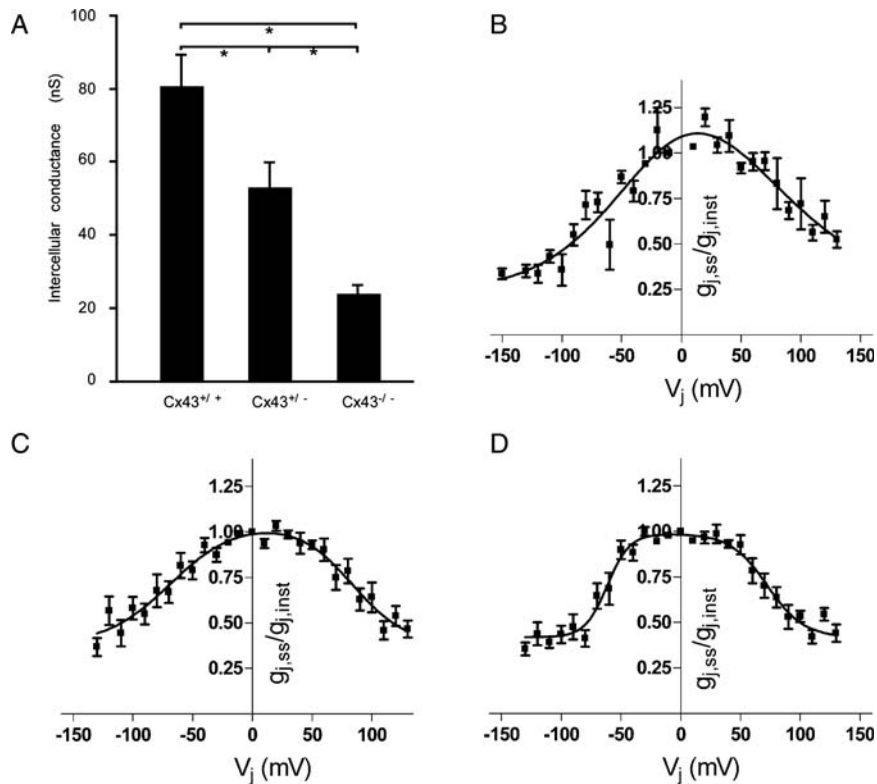


**Figure 2** Change in atrial intercellular electrical conductance,  $g_{j,0}$  and voltage gating with germline Cx43 ablation. (A) Germline ablation of Cx43 decreased intercellular electrical conductance in atrial cell pairs from  $80 \pm 9$  nS ( $n = 17$ ) to  $53 \pm 7$  nS (heterozygous deletion;  $n = 32$ ) and to  $23 \pm 2$  nS (homozygous deletion;  $n = 35$ ). Asterisks denote statistical difference ( $P < 0.01$ ). (B–C) Relative gap junctional conductance ( $g_{j,ss}/g_{j,inst}$ ) in atrial cell pairs [Cx43<sup>+/+</sup>: (B); Cx43<sup>+/-</sup>: (C); Cx43<sup>-/-</sup>: (D)]. With ablation of Cx43, the decrease in  $g_j$  at steady state with increasing transjunctional voltage,  $V_j$ , occurs at higher  $V_j$ , indicating dominance of Cx40 (for numerical analysis, see Table 1).

**Table 1** Gating parameters of Cx43<sup>+/+</sup>, Cx43<sup>+/-</sup>, and Cx43<sup>-/-</sup> gap junctions obtained from the fit of the Boltzmann equation to the relationship between relative intercellular conductance ( $g_{j,ss}/g_{j,inst}$ ) and transjunctional voltage,  $V_j$ , at steady state

	$V_{j,0}$ (mV)	$g_{j,min}$ (norm)	$g_{j,max}$ (norm)
Cx43 <sup>+/+</sup>	-36.6/65.4	0.2	1.07
Cx43 <sup>+/-</sup>	-68.6/83.1	0.38	1.05
Cx43 <sup>-/-</sup>	-61.5/72.3	0.42	0.99

$V_{j,0}$  (mV),  $V_j$  at which 50% of the channels are in the residual state.

full Cx43 ablation was statistically significant with respect to both  $I_{Na}$  in Cx43<sup>+/+</sup> and Cx43<sup>+/-</sup> cells ( $P < 0.05$ ). The average decrease of  $I_{Na}$  with full Cx43 ablation amounted to 55%.

### 3.3. Effects of atrial germline Cx43 ablation on Cx40 and Cx45 immunofluorescence signals in atrial gap junctions

Cx43<sup>+/+</sup>, Cx43<sup>+/-</sup>, and Cx43<sup>-/-</sup> cell pairs were immunostained for Cx43 and Cx45 or for Cx40 and Cx45. DAPI staining for visualization

of nuclei was performed in all series. Figure 5 illustrates the stainings for Cx43 (red) and Cx45 (green) in the left panels and the stainings for Cx40 (red) and Cx45 (green) in the right panels. The upper two panels depict stainings from pairs of Cx43<sup>+/+</sup> genotype, the lower panels from pairs of Cx43<sup>-/-</sup> genotype. A cell pair with the well-defined cell-to-cell boundary is shown in each panel on the top in the X/Y plane, the green cytoplasmic staining represents amplified background fluorescence. The lower parts of the panels depict the 3D surface plots of Cx43, Cx40, and Cx45 immunofluorescence reconstructed after image deconvolution in the Y/Z (sagittal) plane. The surface plots are presented in a semi-transparent mode to enable the detection of co-localization of Cx43 with Cx45, or correspondingly, Cx40 with Cx45. Typically Cx43 and Cx40 are co-localized in large gap junctions. However, smaller junctions often contain Cx43, Cx40, or Cx45 without partner connexin. Genetic ablation of Cx43 is demonstrated by the absence of the respective immunosignals in Figure 5C. These data confirm the observation of heterogeneous Cx composition of atrial gap junctions made in the dual voltage clamp experiments (Figure 3). The analysis of total gap junction immunosignals is illustrated in Figure 6, showing a decrease in both Cx40 and Cx45 immunosignal with Cx43 ablation. In the Cx43<sup>+/-</sup> cell pairs, Cx43, Cx40, and Cx45 decreased to  $46 \pm 7\%$  ( $n = 23$ ),  $58 \pm 13\%$  ( $n = 17$ ), and  $66 \pm 7\%$  ( $n = 16$ ) compared with Cx43<sup>+/+</sup> pairs, respectively. In Cx43<sup>-/-</sup> pairs, Cx40 and Cx45 decreased to  $62 \pm 10\%$  ( $n = 17$ ) and  $66 \pm 8\%$  ( $n = 16$ ), respectively. The decrease in

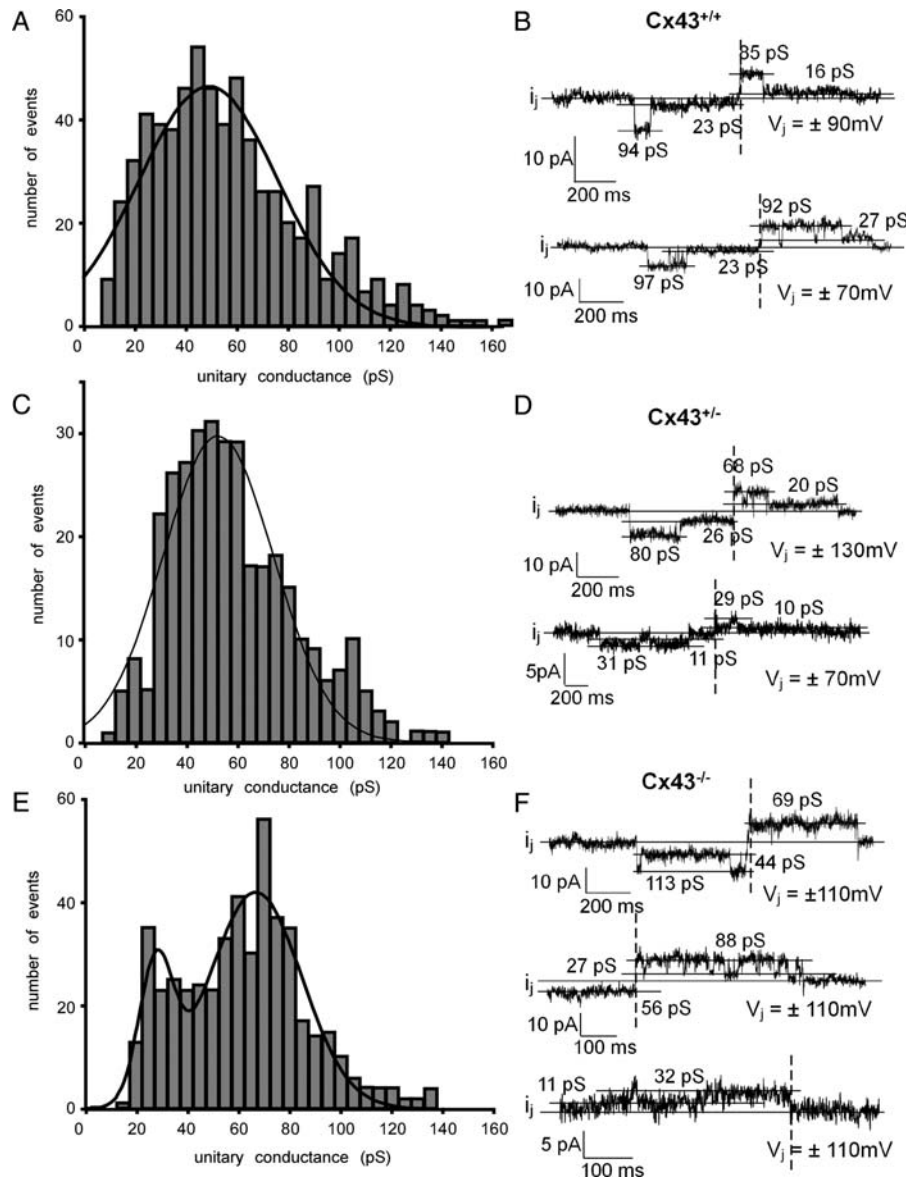


**Figure 3** Change in atrial unitary single gap junction channel conductances,  $\gamma_{ij}$ , with germline Cx43 ablation. (A, C, and D) Frequency histograms of single channel conductances,  $\gamma_{ij,main}$  in Cx43<sup>+/+</sup> (A), Cx43<sup>+/-</sup> (C), and Cx43<sup>-/-</sup> (E) atrial pairs, showing main peaks (Gaussian fit) at  $49 \pm 1.7$  pS (Cx43<sup>+/+</sup>,  $n = 649$ ) to  $53 \pm 1.4$  pS (Cx43<sup>+/-</sup>,  $n = 335$ ), and  $67 \pm 1.8$  pS (Cx43<sup>-/-</sup>,  $n = 481$ ) with a second minor peak appearing at  $27.1 \pm 1.5$  pS. Bin width 5 pS. (B, D, and F) Examples of unitary currents recorded in atrial cell pairs. Vertical dotted line indicates switch of polarity of  $V_j$ .

Cx43, Cx40, and Cx45 immunofluorescence signals in the Cx43<sup>+/-</sup> and Cx43<sup>-/-</sup> pairs with respect Cx43<sup>+/+</sup> was statistically significant ( $P < 0.05$ ), whereas no significant differences were observed between Cx40 and Cx45 signals between the Cx43<sup>+/-</sup> and Cx43<sup>-/-</sup> pairs. A similar decrease of overall Cx40 immunosignal was described in engineered atrial strands with Cx43 ablation.<sup>13</sup>

## 4. Discussion

The present study was undertaken with the aim to define the effect of genetic Cx43 ablation on electrical cell-to-cell conductance in atrial cell pairs, to analyse the change in biophysical properties of the gap junctions and to define potential changes in the partner connexins Cx40 and Cx45. Moreover, our goal was to assess the possibility

that other factors contributing to atrial depolarization and propagation, such Na<sup>+</sup> inward current, might be remodelled by changes in connexin expression. Our study shows three main findings: First, genetic ablation of Cx43 decreases the electrical conductance between atrial myocytes. Secondly, ablation of Cx43 is associated with a decrease in the immunofluorescence signals of the partner connexins Cx40 and Cx45 in gap junctions, and thirdly, Cx43 ablation is associated with a marked decrease in Na<sup>+</sup> inward current.

The presence of three different connexins in atrial myocardium offers a large variety of connexin combinations forming single gap junction channels. Both our high-resolution immunofluorescence analysis and measurements of single channel conductances demonstrate that the Cx43, Cx40, and Cx45 immunosignals in Cx43<sup>+/+</sup> atrial cell pairs and Cx40 and Cx45 signals in Cx43<sup>-/-</sup> pairs reflect the

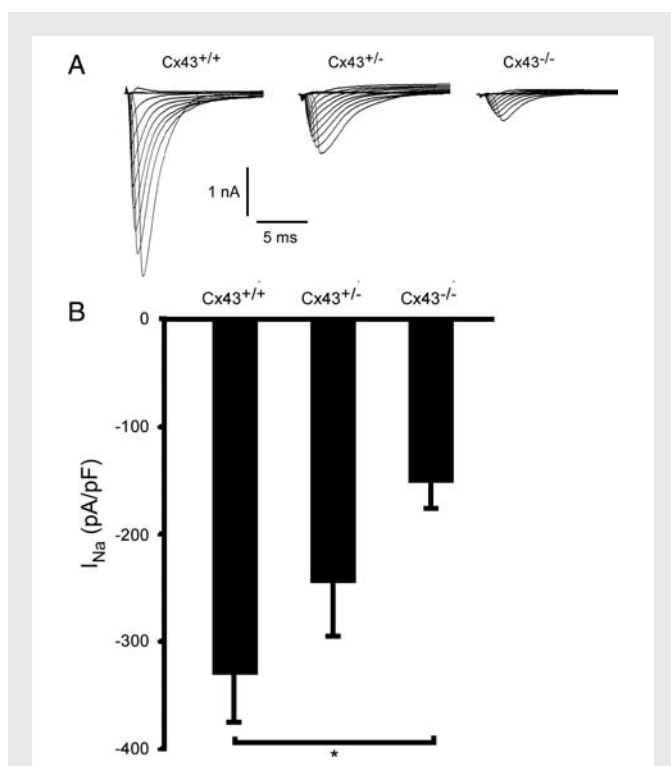


**Figure 4** Change in inward Na current  $I_{Na}$  with germline Cx43 ablation. (A) Original recordings of  $I_{Na}$  recorded in Cx43<sup>+/+</sup> (left), Cx43<sup>+/-</sup> (middle), and Cx43<sup>-/-</sup> (right) atrial myocytes. (B) Peak  $I_{Na}$  density in Cx43<sup>+/+</sup>, Cx43<sup>+/-</sup>, and Cx43<sup>-/-</sup> atrial myocytes. Asterisk denotes statistical significance ( $P < 0.05$ ).

formation of mixed gap junction channels in >70%. In only <30%, homomeric/homotypic channels were identified from voltage clamp sweeps, in which only a single channel opening was observed. This criterion for identification is not fully rigid because even in such a case, the unambiguous attribution of sequential single channel openings to one physical channel is not possible. The electrophysiological measurements were in accordance with the observation that single gap junction plaques were occasionally showing only one distinct connexin immunosignal (Figure 5). A very similar large diversity in the spectrum of single channel conductances was observed in atrial cell pairs from canine<sup>26</sup> and rabbit myocardium.<sup>27</sup> Theoretically, different phosphorylation states could also explain the variety in  $\gamma_j$  values. Although this possibility cannot be ruled out, the previous observation of distinct  $\gamma_j$  peaks in Cx43<sup>+/+</sup> and Cx43<sup>-/-</sup> pairs of ventricular myocytes makes this possibility unlikely.<sup>28</sup> Although the cells were harvested 24 h before birth, we have previously shown that these myocytes mature during 2–4 days in culture and are functionally not distinct from neonatal myocytes after an identical culture period.<sup>13,29</sup> Overall, our measurements of single channel currents indicate the dominating presence of mixed gap junction channels in Cx43<sup>+/+</sup> cell pairs.

Genetic ablation of atrial Cx43 produced changes in electrical intercellular conductance, which reveal multiple complexities of atrial intercellular coupling (i) at the level of the connexin content of single gap junction channels, (ii) connexin regulation and interaction, and (iii) interaction of Cx43 with Na<sup>+</sup> channels.

At the level of the gap junctions, Cx43 ablation produced the expected decrease in intercellular conductance, a shift in the peak

$\gamma_j$  of the single channel histogram from 49pS to 68pS, and a decrease in the voltage gating (increase of  $V_{j,0}$ ), indicating increasing dominance of Cx40. In heterologous expression systems, it has been shown that homomeric/homotypic gap junction channels have a  $\gamma_j$  of 30–40pS (Cx45), 60–120pS (Cx43), and  $\gg 120$  (Cx40), with a  $V_j$ -dependence of voltage gating most expressed in Cx45 channels, being significantly less in Cx43 and even less in Cx40 channels.<sup>24</sup>

Whereas it is not possible to discern the composition of the various mixed gap junction channels from the measurements in Cx43<sup>+/+</sup> and Cx43<sup>+/-</sup> pairs, the results obtained from the Cx43<sup>-/-</sup> pairs, in which only Cx40 and Cx45 are present, suggest the largest population being composed of mixed Cx40/Cx45 channels and a smaller but significant population of homomeric/homotypic Cx45 channels (peak at 29pS). The appearance of this smaller population of Cx45 channels with Cx43 ablation and the shift of the main population towards higher  $\gamma_j$  values may unmask a fraction of channels that also present in the Cx43<sup>+/+</sup> and Cx43<sup>+/-</sup> genotypes, and/or which were forming mixed Cx43/Cx45 channels in the genotypes expressing Cx43. Trafficking of mixed Cx43/Cx45 and Cx40/Cx45 heteromeric connexons would be in line with findings in heterologous expression systems,<sup>24</sup> whereas the formation of heteromeric Cx43/Cx40 connexons is disputed. In one study, Cx43/Cx40 connexons were functional but of significantly lower conductance; in another study, such complexes were identified by co-precipitation but showed no functional correlate.<sup>16,18</sup> Harvesting of cells in our study was strictly limited to the right and the left atrial appendages. This excludes contamination by Cx45 stemming from the sino-atrial or the atrio-ventricular nodes. However, the possibility that the physiological heterogeneity of connexin expression in atrial myocardium<sup>6,30</sup> might have affected our results should be considered.

In accordance with our previous results in synthetic murine strands,<sup>13</sup> the immunofluorescence signal of Cx40 was reduced in gap junctions with Cx43 ablation. In these experiments, we have shown that Cx43 ablation produced a decrease in Cx40, and Cx40 ablation produced an increase in Cx43 in gap junctions. In contrast to junctional connexins, total atrial Cx43 and Cx40 remained unchanged in these experiments. In the present experimental model, it was not possible to fractionate the pools of Cx's into subcellular components due to the limited cell mass provided by the engineered cell pairs. As a new finding, we show that the decrease in Cx45 is closely related to the decrease in Cx40. This finding may have two possible explanations: First, it would confirm that the majority of Cx45 is contained in Cx40/Cx45 hemichannels in a fixed average proportion; secondly; it might reflect the fact that Cx immunofluorescent signals in gap junctions are related to gap junction size,<sup>21</sup> a parameter that is likely to decrease with Cx43 ablation. Currently, we have no explanation why the decrease in Cx40 and Cx45 immunofluorescence was prominent with heterozygous Cx43 ablation and did not further occur with full ablation (Figure 6). In summary, both our previous and the present study suggest that regulation of the atrial connexins embedded into gap junctions is interactive, although the exact mechanisms remain to be elucidated. Trafficking interaction between atrial Cx43 and Cx40 was also suggested from co-expression of mutant Cx43 with normal Cx40 in HeLa cells, where mutant Cx43 produced a decrease in electrical cell-to-cell coupling and internalization of both mutant Cx43 and normal Cx40.<sup>12</sup>

Our finding of an ~50% decrease of inward Na<sup>+</sup> current with germline ablation of Cx43 points to a further complex interaction between multiple proteins expressed in myocardial cell-to-cell

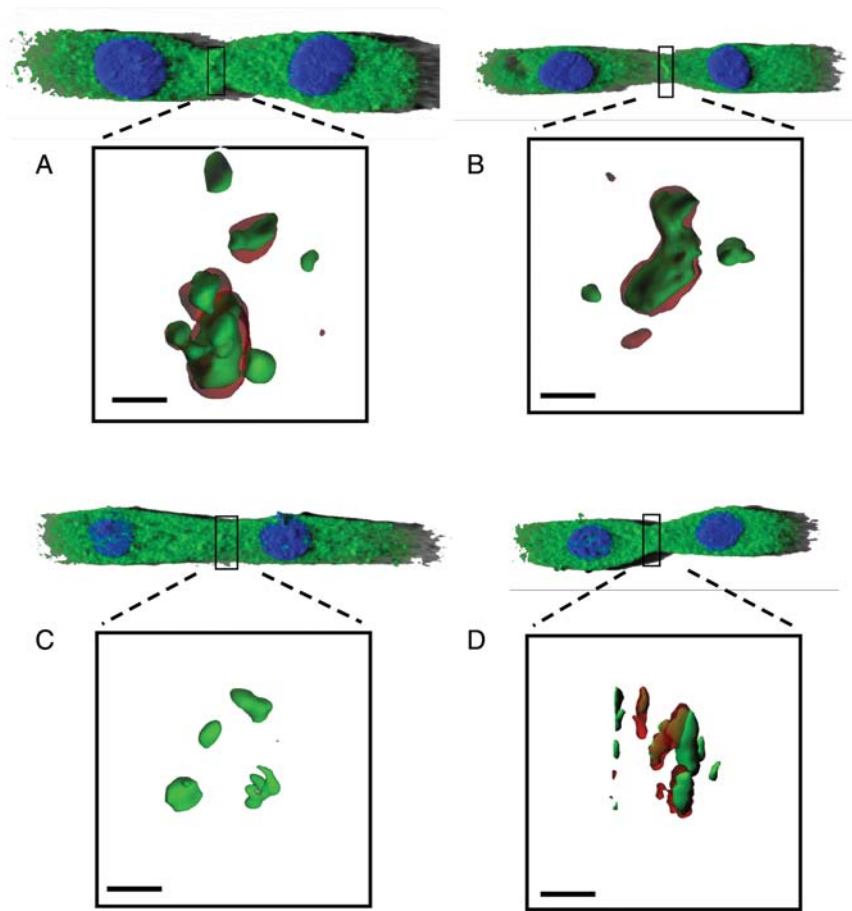


**Figure 5** Changes in Cx43, Cx40, and Cx45 immunosignals in atrial gap junctions with germline Cx43 ablation: Atrial Cx43<sup>+/+</sup> cell pair (A and B), Atrial Cx43<sup>-/-</sup> cell pair (C and D). The top parts of A–D depict a shadow projection view on engineered atrial cell pairs with enhanced cytoplasmic background fluorescence (green) and nuclei (blue). The lower quadrangles of the panels show 3D surface renderings of the immunofluorescence signals in a semi-transparent mode in the z/y (sagittal) plane of the junctions. (A) and (C) show Cx43 immunofluorescence (red) and Cx45 immunofluorescence (green); (B) and (D) show Cx40 immunofluorescence (red) and Cx45 immunofluorescence (green). Scale bars: 10  $\mu\text{m}$ .

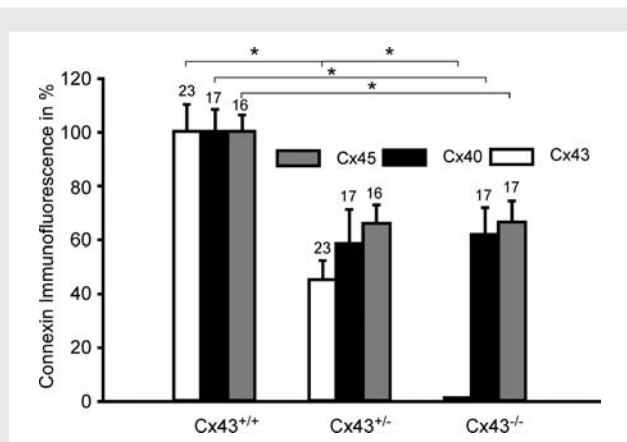


**Figure 6** Changes in Cx43, Cx40, and Cx45 immunosignals in atrial gap junctions with germline Cx43 ablation. The bars with an asterisk denote statistical significance among a given connexin ( $P < 0.05$ ). The Cx43, Cx45, and Cx40 signals are expressed in relative volume, normalized to the respective wild-type. The numbers above the columns denote the number of cell pairs analysed.

junctions belonging to the groups of mechanical junctions, gap junctions, and ion channels, and has implications for arrhythmogenesis. Cardiac sodium channels are located in two distinct compartments with  $\sim 50\%$  of channels being located at the intercalated disc.<sup>1,3,4</sup> Very recently, it has been shown that a reduction of Cx43 in rat ventricular myocytes is associated with a loss in  $\text{Na}^+$  current amplitude.<sup>25</sup> The lack of change in kinetic parameters of  $\text{Na}^+$  flow indicated that this change was due to a reduction in channel density. In the present study, which was carried out in atrial myocytes, total ablation of Cx43 reduced  $\text{Na}^+$  current by  $\sim 50\%$ . These studies and our results suggest that the fraction of  $\text{Na}^+$  channels expressed in the intercalated disc in both ventricle and atrium is modulated by Cx43 expression. At present, it is not possible to provide an exact mechanism for this interaction. However, the observation that different types of connexins and connexins and ion channels interact suggest that regulation of proteins trafficking to the gap junctions share common, yet unknown regulatory principles. Several other studies involving regulation and effects of proteins of mechanical junctions point to such interactions. Thus, human desmosomal mutations decrease both the immunosignal of plakoglobin and Cx43 in gap junctions independently of the type of the mutated desmosomal

protein,<sup>31</sup> and a close association exists at the level of trafficking between an integral chain of protein–protein interactions at the fascia adherens junction and integration of Cx43 into intercalated discs.<sup>32</sup> Genetic ablation of the desmosomal protein plakophilin-2 has been reported to decrease Na<sup>+</sup> inward current,<sup>33</sup> although in this study the decrease in Na<sup>+</sup> current was attributed to a change in kinetics of the Na<sup>+</sup> channels, in contrast to the findings with Cx43 ablation (this study and Ref.<sup>25</sup>).

In conclusion, it is suggested that atrial germline ablation of Cx43 decreases  $I_{Na}$  and electrical intercellular conductance via complex interactions involving trafficking of proteins to the gap junctions. Such a hypothesis is especially interesting because large changes in electrical cell-to-cell coupling alone are required to produce a degree of slow conduction observed in ventricular and atrial arrhythmias. In contrast, theory predicts a high sensitivity of propagation velocity on changes in Na<sup>+</sup> current.<sup>34,35</sup> Thus, changes in atrial connexin expression with associated modulation of Na<sup>+</sup> channel expression may contribute to both, the large range of physiological velocities observed in normal atrium myocardium<sup>36,37</sup> and to propagation slowing in atrial arrhythmias, such as atrial fibrillation. Further studies assessing the molecular mechanisms of cross-talk between mechanical junction proteins, connexins, and ion channel proteins will be required to elucidate this complex behaviour.

## Supplementary material

Supplementary material is available at *Cardiovascular Research* online.

**Conflict of interest:** none declared.

## Funding

Supported by the Swiss National Science Foundation (A.G.K.), the Roche Foundation (A.G.K.), the American Heart Association (MLMcC), and the NIH grant R01 HL079126-01A2 (K.K.P.).

## References

- Kucera JP, Rohr S, Rudy Y. Localization of sodium channels in intercalated disks modulates cardiac conduction. *Circ Res* 2002;**91**:1176–1182.
- Maier SK, Westenbroek RE, McCormick KA, Curtis R, Scheuer T, Catterall WA. Distinct subcellular localization of different sodium channel alpha and beta subunits in single ventricular myocytes from mouse heart. *Circulation* 2004;**109**:1421–1427.
- Maier SK, Westenbroek RE, Schenkman KA, Feigl EO, Scheuer T, Catterall WA. An unexpected role for brain-type sodium channels in coupling of cell surface depolarization to contraction in the heart. *Proc Natl Acad Sci USA* 2002;**99**:4073–4078.
- Petitprez S, Zmoos AF, Ogronnik J, Balse E, Raad N, El-Haou S et al. SAP97 and dystrophin macromolecular complexes determine two pools of cardiac sodium channels Nav1.5 in cardiomyocytes. *Circ Res* 2011;**108**:294–304.
- Severs NJ, Bruce AF, Dupont E, Rothery S. Remodelling of gap junctions and connexin expression in diseased myocardium. *Cardiovascular Res* 2008;**80**:9–19.
- Vozzi C, Dupont E, Coppen SR, Yeh HI, Severs NJ. Chamber-related differences in connexin expression in the human heart. *J Mol Cell Cardiol* 1999;**31**:991–1003.
- von Maltzahn J, Kreuzberg MM, Matern G, Euwens C, Hoher T, Worsdorfer P et al. C-terminal tagging with eGFP yields new insights into expression of connexin45 but prevents rescue of embryonic lethal connexin45-deficient mice. *Eur J Cell Biol* 2009;**88**:481–494.
- Kanter HL, Laing JG, Beyer EC, Green KG, Saffitz JE. Multiple connexins colocalize in canine ventricular myocyte gap junctions. *Circ Res* 1993;**73**:344–350.
- Gourdie RG, Severs NJ, Green CR, Rothery S, Germroth P, Thompson RP. The spatial distribution and relative abundance of gap-junctional connexin40 and connexin43 correlate to functional properties of components of the cardiac atrioventricular conduction system. *J Cell Sci* 1993;**105**(Pt 4):985–991.
- Polontchouk L, Haefliger JA, Ebelt B, Schaefer T, Stuhlmann D, Mehlhorn U et al. Effects of chronic atrial fibrillation on gap junction distribution in human and rat atria. *J Am Coll Cardiol* 2001;**38**:883–891.

- van der Velden HM, Wilders R, Jongsma HJ. Atrial fibrillation-induced gap junctional remodeling. *J Am Coll Cardiol* 2002;**39**:1709; author reply 1709–1710.
- Thibodeau IL, Xu J, Li Q, Liu G, Lam K, Veinot JP et al. Paradigm of genetic mosaicism and lone atrial fibrillation: physiological characterization of a connexin 43-deletion mutant identified from atrial tissue. *Circulation* 2010;**122**:236–244.
- Beauchamp P, Yamada KA, Baertschi AJ, Green K, Kanter EM, Saffitz JE et al. Relative contributions of connexins 40 and 43 to atrial impulse propagation in synthetic strands of neonatal and fetal murine cardiomyocytes. *Circ Res* 2006;**99**:1216–1224.
- Desplantez T, Dupont E, Severs NJ, Weingart R. Gap junction channels and cardiac impulse propagation. *J Membr Biol* 2007;**218**:13–28.
- Harris AL. Emerging issues of connexin channels: biophysics fills the gap. *Q Rev Biophys* 2001;**34**:325–472.
- Cottrell GT, Burt JM. Functional consequences of heterogeneous gap junction channel formation and its influence in health and disease. *Biochim Biophys Acta* 2005;**1711**:126–141.
- Cottrell GT, Burt JM. Heterotypic gap junction channel formation between heteromeric and homomeric Cx40 and Cx43 connexons. *Am J Physiol Cell Physiol* 2001;**281**:C1559–C1567.
- Valiunas V, Gemel J, Brink PR, Beyer EC. Gap junction channels formed by coexpressed connexin40 and connexin43. *Am J Physiol Heart Circ Physiol* 2001;**281**:H1675–H1689.
- Geisse NA, Sheehy SP, Parker KK. Control of myocyte remodeling *in vitro* with engineered substrates. *In Vitro Cell Dev Biol Anim* 2009;**45**:343–350.
- Desplantez T, Halliday D, Dupont E, Weingart R. Cardiac connexins Cx43 and Cx45: formation of diverse gap junction channels with diverse electrical properties. *Pflügers Arch* 2004;**448**:363–375.
- McCain M, Desplantez T, Geisse N, Rothen-Rutishauser B, Oberer H, Parker K et al. Cell-to-cell coupling in engineered pairs of rat ventricular cardiomyocytes: relation between Cx43 immunofluorescence and intercellular electrical conductance. *Am J Physiol Heart Circ Physiol* 2012;**302**:H443–H450.
- Van Rijen HV, Wilders R, Van Ginneken AC, Jongsma HJ. Quantitative analysis of dual whole-cell voltage-clamp determination of gap junctional conductance. *Pflügers Arch* 1998;**436**:141–151.
- Chen-lzu Y, Moreno AP, Spangler RA. Opposing gates model for voltage gating of gap junction channels. *Am J Physiol Cell Physiol* 2001;**281**:C1604–C1613.
- Moreno AP. Biophysical properties of homomeric and heteromultimeric channels formed by cardiac connexins. *Cardiovascular Res* 2004;**62**:276–286.
- Jansen JA, Noorman M, Musa H, Stein M, de Jong S, van der Nagel R et al. Reduced heterogeneous expression of Cx43 results in decreased Nav1.5 expression and reduced sodium current that accounts for arrhythmia vulnerability in conditional Cx43 knockout mice. *Heart Rhythm* 2011 Nov 16. [Epub ahead of print].
- Elenes S, Rubart M, Moreno AP. Junctional communication between isolated pairs of canine atrial cells is mediated by homogeneous and heterogeneous gap junction channels. *J Cardiovasc Electrophysiol* 1999;**10**:990–1004.
- Verheule S, van Kempen MJ, te Welscher PH, Kwak BR, Jongsma HJ. Characterization of gap junction channels in adult rabbit atrial and ventricular myocardium. *Circ Res* 1997;**80**:673–681.
- Beauchamp P, Choby C, Desplantez T, de Peyer K, Green K, Yamada KA et al. Electrical propagation in synthetic ventricular myocyte strands from germline connexin43 knockout mice. *Circ Res* 2004;**95**:170–178.
- Thomas SP, Bircher-Lehmann L, Thomas SA, Zhuang J, Saffitz JE, Kleber AG. Synthetic strands of neonatal mouse cardiac myocytes: structural and electrophysiological properties. *Circ Res* 2000;**87**:467–473.
- Bagwe S, Berenfeld O, Vaidya D, Morley GE, Jalife J. Altered right atrial excitation and propagation in connexin40 knockout mice. *Circulation* 2005;**112**:2245–2253.
- Asimaki A, Tandri H, Huang H, Halushka MK, Gautam S, Basso C et al. A new diagnostic test for arrhythmogenic right ventricular cardiomyopathy. *N Engl J Med* 2009;**360**:1075–1084.
- Shaw RM, Fay AJ, Puthenveedu MA, von Zastrow M, Jan YN, Jan LY. Microtubule plus-end-tracking proteins target gap junctions directly from the cell interior to adherens junctions. *Cell* 2007;**128**:547–560.
- Sato PY, Musa H, Coombs W, Guerrero-Serna G, Patino GA, Taffet SM et al. Loss of plakophilin-2 expression leads to decreased sodium current and slower conduction velocity in cultured cardiac myocytes. *Circ Res* 2009;**105**:523–526.
- Shaw RM, Rudy Y. Ionic mechanisms of propagation in cardiac tissue. Roles of the sodium and L-type calcium currents during reduced excitability and decreased gap junction coupling. *Circulation Res* 1997;**81**:727–741.
- Kleber AG, Rudy Y. Basic mechanisms of cardiac impulse propagation and associated arrhythmias. *Physiol Rev* 2004;**84**:431–488.
- Kanagaratnam P, Rothery S, Patel P, Severs NJ, Peters NS. Relative expression of immunolocalized connexins 40 and 43 correlates with human atrial conduction properties. *J Am Coll Cardiol* 2002;**39**:116–123.
- Kleber AG, Janse MJ, Fast VG. Normal and abnormal conduction in the heart. In: *The Handbook of Physiology, The Cardiovascular System*, Vol. 1. *The Heart* American Physiological Society, Oxford University Press; 2001. p455–529.